ANALYSIS OF OPTIMUM CONDITIONS FOR HIGH ORDER HARMONIC GENERATION IN GASEOUS MEDIAS

Mihai STAFE[1], Constantin NEGUȚU[2], Georgiana C. VASILE[3], Niculae N. PUȘCAȘ[4]

In this article we present a theoretical analysis of high order harmonic generation (HHG) in gas jets with high intensity laser pulses. We estimate several laser and target parameters (i.e. focusing parameters- focus length, beam radius at the waist, length of the nonlinear medium, and concentration of the gas jet) involved in efficient conversion of a Nd^{3+}:YAG nanosecond laser radiation to higher frequencies.

First, we evaluate the wave vector mismatches, length of the nonlinear medium and focusing parameters for efficient generation of the fifth and seventh order harmonics generated in mixtures of sodium vapors and xenon. The theoretical findings are in good agreement with the experimental results published in the literature.

Second, in the case where the gas jet is produced by laser ablation, the condition for obtaining optimum gas density profile for HHG is evaluated by solving numerically the hydrodynamics of the ablation jet produced by a nanosecond laser pulse.

Keywords: high order harmonic generation, conversion gaseous jet, ablation plasma.

1. Introduction

The properties of a material change due to the nonlinear effects which occur when the high power laser radiation, characterized by electric field intensities around $10^6 \div 10^7$ V/cm or higher (which are comparable to the atomic electric field), interacts with the material [1-3]. In the last years, high-order harmonic generation has become a leading research field in nonlinear optics as a way to produce coherent extreme ultraviolet (XUV, 100-10 nm) and soft-X radiation, as well as attosecond pulses. The production of vacuum-ultraviolet (VUV, 200-100 nm) and XUV coherent radiation with ultra-short duration

[1] Lecturer, Physics Department, University POLITEHNICA of Bucharest, Romania, e-mail: stafe@physics.pub.ro
[2] Lecturer, Physics Department, University POLITEHNICA of Bucharest, Romania, e-mail: negutu@physics.pub.ro
[3] Lecturer, Physics Department, University POLITEHNICA of Bucharest, Romania
[4] Professor, Physics Department, University POLITEHNICA of Bucharest, Romania

through the process of high harmonic generation (HHG) becomes a current practice [1, 2]. The high harmonic radiation can be used for various applications such as optical lithography and pump-probe experiments at natural atomic time scale.

The high order harmonic ultra-short pulses are produced by focusing near-infrared and visible laser pulses in different types of materials: gases, liquids, solids, laser-generated plasmas, ablated nanoparticles etc. The generation efficiency decreases rapidly with the harmonic order [1-8]. In isotropic (centro-symmetric) media (e.g. gases), for symmetry reasons only odd harmonics are produced, with efficiencies up to 50%.

HHG in gas jets requires pulses of high intensities (typically 10^{14}–10^{15} W/cm^2) which can easily be achieved with fs driving lasers. Lower order harmonics in the vacuum ultraviolet (VUV) domain can be even generated by using nanosecond laser pulses. Since the beginning of HHG studies, ions from the laser ablation plasmas have been investigated as alternative isotropic media to the ordinary gas jets targets for HHG [11-16]. The idea was that, since ions have higher ionization potentials as compared to the neutral noble gas atoms, the harmonic cutoff should extent toward shorter wavelengths. However, the ionization leads to self-induced defocusing of the fundamental laser beam, having a detrimental effect on the HHG process.

Laser ablation can easily generate ionic and neutral species [17–20, 26, 27], together with microclusters and nanoparticles [21-23], with various densities and optical properties that can in principle be controlled by the right choice of solid target and laser wavelength and pulse duration [24, 25].

Experimental and theoretical studies on HHG showed that the right control of the two limiting factors of conversion efficiency (self-defocusing and wave phase mismatch between the harmonics and the converting radiation) leads to efficient HHG in weakly ionized ablation plasmas (ionization degree <5%) produced on metallic targets [11, 13]. The main goals of these studies are: increase of the highest harmonic order, the appearance of a plateau in the spectrum of high-order harmonics, the high yield of HHG achieved with plasma formation, the realization of resonance-induced enhancement of individual harmonics, the efficient harmonic enhancement for cluster containing plasma plumes, etc.

Here we present an analysis of high order harmonic generation in gaseous jets, evaluating several parameters for the high conversion efficiency, such as: wave vector mismatches, length of the nonlinear medium and focusing parameters (i.e. focus length and beam radius at the waist). Additionally, we propose to analyze the properties of the ablation plumes (as HHG conversion mediums) produced with low intensity nanosecond laser pulses on Al targets in vacuum.

The paper is organized as follows: in Sec. 2-3 we present some theoretical considerations, and in Sect. 4 we discuss the simulation results concerning the evaluation of several parameters in order to obtain the highest conversion efficiency. In Sect. 5 we outline our conclusions concerning the results.

2. Theoretical prediction of phase matching for HHG

At low laser intensities (i.e. up to 10^{13} W/cm^2), the description of low-order harmonic generation process can be performed in terms of polarization $\vec{P}$ which is induced in the nonlinear medium by the laser field itself. Polarization can be developed in power (Taylor) series of the applied laser field $\vec{E}$, in the form:

$$\vec{P} = \varepsilon_0 \chi^{(1)} \vec{E} + \varepsilon_0 \chi^{(2)} \vec{E}^2 + \varepsilon_0 \chi^{(3)} \vec{E}^3 + ... \quad (1)$$

The first term, which includes the first order susceptibility $\chi^{(1)}$, characterizes the linear propagation of the electromagnetic waves and describes the linear optical properties through the refractive index. The other terms, which include nonlinear susceptibilities $\chi^{(2)}, \chi^{(3)}, ..., \chi^{(n)}$ describe the propagation of the electromagnetic waves in media in which nonlinear effects occur. The coefficients $\chi^{(j)}$ (called the j-th order susceptibilities) are tensors of the order j+1, representing both the polarization dependent nature of the parametric interaction as well as the symmetry of the nonlinear material [1,2]. For gas media, which are isotropic, and linearly polarized light they reduce to scalar quantities.

A perturbative solution of Maxwell's equations can be obtained considering the linearly polarized laser beam as a series of harmonics of the fundamental frequency ω_1 as:

$$E(\vec{r},t) = \sum_{j=1}^{n} E_j(\vec{r},t) = \sum_{j=1}^{n} A_j(\vec{r}) exp\left[-i(\omega_j t - k_j z)\right] + c.c., \quad (2)$$

where $\omega_n = n\omega_1$ with n positive integer and A_j are the complex amplitude. The pump field $(n=1)$ is always much more intense than the harmonic field, so that the total electric field in Eq. (2) can be replaced by the fundamental field alone. In centro-symmetric media, the even terms in the power series vanish due to symmetry reasons (also related to parity conservation in multi-photon processes), and the nonlinear part of the polarization reduces to:

$$\vec{P}^{nl} = \sum_{j=1}^{n} \vec{P}_j(\vec{r},t) = \varepsilon_0 \sum_{j=1}^{n} \chi^{(j)} E_1^{\,j}(\vec{r},t), \quad (3)$$

with j odd integer. In the case of slowly-varying-amplitude approximation (i.e. variation of the electric field amplitude j occurs only over distances much larger

than an optical wavelength), the wave equation for the j-th harmonic field can be written as:

$$2ik_j \frac{\partial A_j(\vec{r})}{\partial z} + \nabla_T^2 A_j(\vec{r}) = -\frac{\omega_j^2}{c^2} \chi^{(j)} A_1^j(\vec{r}) exp(i\Delta k_j z), \tag{4}$$

where

$$\gamma_i = \frac{\sigma_i}{2}\sqrt{\frac{\mu_0}{\varepsilon}},\ K = \frac{\varepsilon_0}{2}\sqrt{\frac{\mu_0}{\varepsilon}}\chi_{\alpha_1\alpha_2\alpha_3},\ \Delta k = k_1 - k_2 - k_3, \tag{5}$$

is the wave vector mismatch. Considering a Gaussian laser beam, the fundamental electric field can be expressed in the form [2]:

$$A_1(r) = A_{10} \frac{\exp\left[-\frac{R^2}{w_0^2(1+i\xi)}\right]}{1+i\xi}, \tag{6}$$

where

$$R = \sqrt{x^2 + y^2} \tag{7}$$

represents the cylindrical radial coordinate,

$$\xi = \frac{2z}{b} \tag{8}$$

is a normalized coordinate along the z axis with the zero set at the beam waist,

$$b = \frac{2\pi w_0^2}{\lambda} \tag{9}$$

is the beam confocal parameter, w_0 is the beam radius at the waist (Fig. 1), and A_{10} is the electric field amplitude at $\xi = 0$ and $R = 0$.

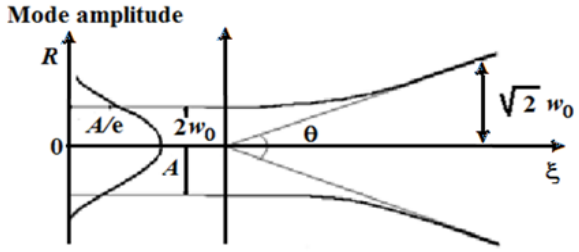

Fig. 1. The Gaussian beam parameters.

By integrating Eq. (4) in the case of a Gaussian beam given by Eq. (6) one can obtain the generated electric field amplitude of the n-th harmonic in the form:

$$A_n(r) = \frac{2\pi i n \omega_1}{n_0 c} \chi^{(n)} F_n(\Delta k_n, z_0, z) A_{10}^n \frac{exp\left[-\frac{nR^2}{w_0^2(1+i\xi)}\right]}{1+i\xi}, \quad (10)$$

where n_0 represents the linear index of refraction of the medium, and

$$F_n(\Delta k_n, z_0, z) = \int_{z_0}^{z'} \frac{\exp(i\Delta k_n z')}{\left(1+\frac{2iz}{b}\right)^{n-1}} dz' \quad (11)$$

is the so-called phase matching integral, which describes the effect of de-phasing between the harmonic wave and its source polarization. In Eq. (11) z_0 and z represent the starting and ending coordinates of the interaction region respectively.

The intensity of the generated harmonic radiation is given by:

$$I_n(r) = 2N\sqrt{\frac{\mu_0}{\varepsilon_0}}|A_n(r)|^2 = \frac{8\pi^2 n^2 \omega_1^2}{n_0 c^2}\sqrt{\frac{\mu_0}{\varepsilon_0}}\left|\chi^{(n)}\right|^2 \left|F_n(\Delta k_n, z_0, z)\right|^2 A_{10}^{2n} \frac{\left|exp\left[-\frac{nR^2}{w_0^2(1+i\xi)}\right]\right|^2}{1+i\xi^2} \quad (12)$$

Here, N represent the particle density. From Eq. (12) one observe that the peak intensity of the n-th harmonic $I_n(0)$ is proportional to the n-th power of the peak intensity of the fundamental beam, $I_1(0) \sim A_{10}^2$. In principle, at sufficiently high pump powers the higher order harmonics could be produced more efficiently than the lower ones. However, the perturbative description is no longer valid at very high intensities comparable to the atomic electric field. Also, $I_n(0)$ is proportional to the square of the n-th order nonlinear susceptibility, $\left|\chi^{(n)}\right|^2$.

To achieve optimum energy conversion from the pump beam to the harmonic beam the field strength E_n has to stay in phase with its source polarization, P_n. Calculation of the phase matching integral $F_n(\Delta k_n, z_0, z)$ given by Eq. (11) shows a strong dependence of the conversion efficiency on the focusing condition.

In the case of a long focus (i.e. $b >> |z|$, $|z_0|$), as in usual experiments employing gas jets, the phase matching integral approaches the sinc^2 function, typical of the phase matching for plane-waves, where maximum efficiency is achieved at $\Delta k_n \sim 0$. In this configuration, harmonic generation is allowed for both negative and positive values of the wave vector mismatch.

In the case of tight-focusing of the laser beam (i.e. $b << |z|, |z_0|$) which is typical for low-order harmonic generation in cells, F_n has a maximum for positives values of Δk_n, and is zero for $\Delta k_n \geq 0$. This peculiar behavior can be understood in terms of on-axis space-dependent phase shift $\tan^{-1}(2z/b)$ between a Gaussian beam and a plane wave beam. Because of the phase, there is a change in the sign of the phase lag between the field E_n and the polarization P_n when passing though the beam focus.

As a consequence, the harmonic field generated in first half of the interaction region would be converted back to the pump beam in the second half, if no compensating wave vector mismatch is present. An important consequence of this behavior is that third-harmonic generation process is not possible in a positive (or normal) dispersive medium, like single component gases far from resonances.

As shown by Eq. (12), there are basically three possibilities to increase the low-order harmonic generation efficiency, namely: a) optimum phase matching, b) high-intensity fundamental beam at low wavelengths (in UV domain), and c) resonant enhancement.

In what follows, we present briefly these three situations.

a) Phase matching optimization of the low-order harmonic generation in gases is strongly dependent on the focusing condition. In practical situations, the fundamental beam has to be focused in order to achieve sufficiently high intensity in the interaction region and, at the same time, it has to avoid damage on the optics by the high energy of the pump pulses. Optimum phase matching in this situation is achieved in negatively dispersive or dispersion less media. This is not in general the case for single component gases, but specific gas mixtures can be used to achieve optimum phase matching. For example, a cell containing mixture of normally dispersive argon and negatively dispersive cadmium vapor was used to produce phase-matched VUV radiation. However, this phase matching condition is difficult to control when using a gas jet as nonlinear medium, which is the usual experimental situation. Moreover, since phase matching is by its nature wavelength-dependent, there are fundamental limitations when tunable radiation is used.

b) The production of tunable narrow-band VUV/XUV radiation via low-order harmonic generation requires the use of a tunable narrow-band high-intensity fundamental UV beam. The lack of primary sources in the UV can be overcome by frequency doubling intense visible pulses. Such laser source was developed in the late 1980's by combining the pulsed-dye-amplification technique with harmonic generation in gases. Due to the fast decay rate of dyes (nanoseconds for visible dyes, and even hundreds of picosecond for near-infrared dyes) the production and subsequent amplification of a laser pulse in dye cells enables the

generation of energetic pulses that follow the temporal characteristic of the pump pulses. So, pulsed amplification of a cw tunable seeding beam by a single-mode pump laser with a smooth pulse time profile and a stable intensity, e.g., from an injection-seeded Q-switched laser, enables the generation of energetic visible pulses with a Fourier transform limited frequency spectrum.

c) The nonlinear response of a medium, i.e., its nonlinear susceptibility, is enhanced when the pump frequency meets a (multi-photon) resonant transition. However, the production of tunable radiation via a resonant scheme is not possible using only one pump frequency, like in third-harmonic generation, since the resonant condition cannot be kept while tuning the pump frequency. On the other side, efficient production of tunable VUV radiation is possible using resonantly enhanced four-wave-mixing schemes: one fixed frequency, ω_1, matches an atomic transition, and mixes with another tunable frequency, ω_2, in order to generate tunable radiation. In the last years resonantly enhanced four-wave mixing has been extensively studied in atomic vapors, molecular gases and noble gases. The electromagnetically-induced transparency phenomenon can lead to enhancement of the efficiency in this wave-mixing scheme.

The electromagnetic emission by an atom exposed to a laser field of intensity above the perturbative regime cannot be described in terms of the atomic polarization and substantial ionization may occur during the laser pulse leading to a plasma formation. In a plasma, ion-electron pairs give the dominant contribution to the electromagnetic emission, which comes essentially in two forms: incoherent and coherent Bremssthralung radiation in a plasma generates an isotropic incoherent continuum at short wavelength ($\lambda \leq 30$ nm).

The interaction of more intense laser pulses (intensity $I \geq 10^{13}$ W/cm^2) with atoms and molecules leads to several multi-photon, non-perturbative phenomena such as high-order harmonic generation and above threshold ionization.

3. Theoretical model for characterization of the ablation plume conversion medium

The laser-ablation plasmas have been investigated as alternative conversion medium to the ordinary gas jets targets for HHG. The idea behind these studies was that, since ions have higher ionization potentials as compared to the neutral noble gas atoms, the harmonic cutoff should extent toward shorter wavelengths. However, the ionization leads to self-induced defocusing of the fundamental laser beam, having a detrimental effect on the HHG process. Experimental and theoretical studies showed that, by controlling the two limiting factors of HHG efficiency (self-defocusing and wave phase mismatch between the harmonics and the driving laser radiation), one can generate efficiently high

harmonics in weakly ionized ablation plasmas produced on metallic targets [16, 11].

Here we propose to analyze the properties of the ablation plume medium produced with low intensity nanosecond laser pulses on Al targets in vacuum. The calculation of spatial profile of the ablation plasma density at different moments is very important for efficient HHG, enabling prediction of the positioning and timing of the HHG driving laser pulse within the conversion ablation plume to obtain phase matching conditions.

The low ionization ablation plasma produced by a ns laser pulse, at fluences of the order of 10 J/cm^2, is a result of the target evaporation and ionization induced mainly by the absorption of the laser energy by the free electrons via inverse Bremsstrahlung. The absorbed energy relaxes at picosecond scale via electron-electron and electron-phonon collisions.

Thus, the temperature distribution in the axial direction within the target can be determined from the 1D heat equation when the thermal penetration depth of target is much smaller than the laser spot diameter on the target surface. Theoretical description of the heating process is presented in previous works [25,28,17,18,24,29]. Here we emphasize the main characteristics of the theoretical model regarding the dynamics of the ablation plume.

Ionization degree of the ablation plume produced at fluences of the order of 10 J/cm^2 is very low (~several percent), and thus the absorption of the laser beam within the ablation plume is negligible, as indicated by our previous experimental findings [18]. Due to expansion of the evaporated layer near the target surface, the plasma temperature and density at the outer limit of the Knudsen layer are smaller than the equilibrium values [25]:

$$T = 0.67 T_s \text{ and } N = 0.31 \frac{p_{sat}}{k_B T_s}, \tag{13}$$

where T_s is the temperature of the target surface. The recession velocity of the melt surface due to evaporation is given by the Hertz-Knudsen equation

$$v_a = \frac{1}{\rho_t} \left(\frac{m}{2\pi k_B T_s} \right)^{1/2} (p_{sat} - p_{part}). \tag{14}$$

Here,

$$p_{sat} = p_0 \exp\left[\frac{\Delta H_{lv}}{R} \left(\frac{1}{T_b} - \frac{1}{T_s} \right) \right], \tag{15}$$

is the saturated vapour pressure given by the Clausius-Clapeyron relation, ΔH_{lv} is the enthalpy of vaporization per mol at the normal boiling point T_b [25], ρ_t denotes the mass density of the target, m is the Al atom mass, and $p_0 = 1$ atm is

the normal pressure. p_{part} is the partial pressure of Al vapors taken as an instant average pressure over the ablation plume. The thermal and optical properties of Al are taken from [25]. The boundary and initial conditions of the heat equation are determined by Eq. (13) and the ambient conditions [25,17].

The dynamics of the quasi-equilibrium ablation plume beyond the Knudsen layer can be described by the 1D Euler equations (describing conservation of mass, momentum and energy in the plume domain) when the laser spot diameter is large [25,30,31]:

$$\frac{\partial \rho}{\partial t} = -\frac{\partial (\rho v)}{\partial x} \tag{16}$$

$$\frac{\partial (\rho v)}{\partial t} = -\frac{\partial (\rho v^2 + p)}{\partial x} \tag{17}$$

$$\frac{\partial (\rho \varepsilon + \rho v^2 / 2)}{\partial t} = -\frac{\partial (\rho v \varepsilon + pv + \rho v^3 / 2)}{\partial x}. \tag{18}$$

Here, ρ is the plume mass density, v is the local plume velocity, and $p = \rho k_B T / m$ is the local pressure in the ideal gas approximation. Since we are interested in the low laser fluences regime, where the vapor is weakly ionized, we neglected the plume absorption and radiation so that the internal energy density of the plume can be written as $\rho\varepsilon = \frac{3}{2}\frac{\rho}{m}k_B T$.

The target domain in the axial direction, where the heat equation is solved, is ~10 microns (much larger than the thermal penetration depth) and was discretized into a non-uniform grid with the high density nodes near the target surface, the minimum grid cell being ~1 nm. The ablation plume domain in the axial direction, where the Euler equations are solved, is ~5 mm (so that any disturbance in the domain cannot reach the furthest boundary from the surface) and was also discretized into a non-uniform grid with the high density nodes near the target-plume interface, the minimum grid cell being 50 nm. The limit x=0 of the plume domain corresponds to the outer limit of the Knudsen layer so that the density and temperature of the plume at x=0 boundary are given by Eq. (13). The plume velocity at x=0 is derived from the mass flow continuity condition at the target- plume interface:

$$\rho v = \rho_t v_a. \tag{19}$$

The boundary conditions at x=5 mm and the initial conditions of Eq. (16-18) are determined by Eq. (13-15) and (19) with T_s=300 K.

The total integration time is ~20 ns, beyond the duration of the laser pulse, with a minimum time cell of $\sim 10^{-12}$ s. The heat equation and the hydrodynamics equations are integrated in a multi-step method by using the standard finite

elements method implemented in MATLAB by which partial differential equations are transformed into ordinary differential equations using a second-order accurate spatial discretization [32]. The number of integration time steps is ~2000. The small time steps fulfill convergence conditions of the solutions, simultaneously for the heat equation and hydrodynamics equations [33]. The solutions of the hydro-equations are smoothed after each integration step.

The two parts of the model (i.e. heat equation and Euler equations) are strongly connected. Thus, the outputs of every integration step of the heat equation (such as temperature of the target surface and evaporation velocity, plume temperature, density and velocity at the outer limit of Knudsen layer) give boundary conditions for the Euler equations.

On the other hand, the Euler equations give the partial pressure of Al vapors in the ablation plume which influences the evaporation speed (see Eq. (17)) and the vapor back-flux onto the target surface which leads to the re-condensation phenomenon.

4. Results and discussion

Based on the models presented in Section 2 ([1, 3, 4, 7]), considering a driving laser beam with a Gaussian intensity profile in the radial direction, we evaluated several geometrical irradiation parameters for which one can obtain the maximum power of the fifth and seventh harmonic.

In the case of a long focus, the intensity of the fifth harmonic radiation (Eq. 12) reaches its maximum for $\frac{b}{L}=\frac{1}{2}$, where L is the length of the nonlinear medium (Fig. 2) if the wave vector mismatch for the direct fifth harmonic generation process Δ_{15} and that corresponding to the step processes involving third harmonic generation Δ_{13} are both of them zero ($\Delta_{15}=\Delta_{13}=0$).

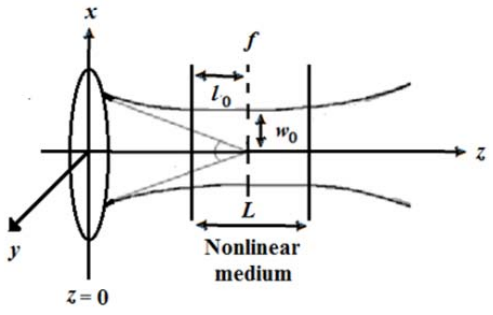

Fig. 2. The propagation of the Gaussian beam through the nonlinear medium.

In the case of tight-focusing of the laser beam considering that the beam is focused in the center of the nonlinear medium $\Delta_{15} = \frac{6}{b}$ for the direct fifth harmonic generation process and $\Delta_{15} = 2\Delta_{13} = \frac{4}{b}$ for that corresponding to the step processes involving third harmonic generation process.

The above mention conditions may be obtained using gaseous mixtures like: alkali metal vapors (e. g. sodium) and noble gases as buffer (e. g. xenon) with suitable concentrations, $\frac{N_{Xe}}{N_{Na}}$, suitable length of the nonlinear medium, and focusing parameters (focus length, beam radius at the waist).

In the case of a laser radiation with $\lambda = 1.06\,\mu$m (Nd^{3+}:YAG) and 2.5×10^{8} W pump power, $\frac{N_{Xe}}{N_{Na}} = 31.2$, focus length of about 28 cm the above mentioned calculated parameters are in good agreement with the experimental results being obtained a fifth harmonic radiation with 4 kW power and an efficiency about 5×10^{-6} [8].

The above mention parameters were evaluated in the case of seventh harmonic generation process.

In the case of a long focus the intensity of the seventh harmonic radiation (Eq. 12) reaches its maximum for $\frac{b}{L} = \frac{1}{2}$, where L is the length of the nonlinear medium (Fig. 2) if the wave vector mismatch for the direct seventh harmonic generation process Δ_{17} and that corresponding to the step processes involving fifth harmonic generation Δ_{15} are both of them zero ($\Delta_{17} = \Delta_{15} = 0$).

In the case of tight-focusing of the laser beam considering that the beam is focused in the center of the nonlinear medium $\Delta_{15} = \frac{10}{b}$ for the direct seventh harmonic generation process and $\Delta_{17} = \frac{4}{b}$ for that corresponding to the step processes involving fifth harmonic generation process. The above mentioned evaluated parameters are in good agreement with the experimental results obtained in the seventh order harmonic generation [8].

In order to determine the optimum timing for sending the intense driving laser pulse through the non-linear conversion medium, we run simulations based on model presented in Section 3 to find properties of the ablation plume conversion medium. This is because the harmonics intensity is a function of gas density (see Eq. (12)).

The fluence of the focused ablation laser pulse (4.5 ns, 1064 nm) was set to 15 J/cm^2, which gives a peak intensity of ~3GW/cm^2 at the Al target surface. These parameters determine a high density ablation plume, above 10^{19} cm^{-3} as needed in most HHG in gas jets where backing pressure of several bars are used ([34,35], and low ionization degree (less than 1% as estimated experimentally [18]).

The Gaussian temporal profile of the laser pulse is presented in Fig. 3(a) whereas the temporal evolution of the temperature of target surface is presented in Fig. 3(b). The peak temperature of the target surface is ~6000 K, slightly below the critical point of Al [36], and is reached at ~10 ns, which very close to the 9 ns when the peak of the laser pulse intensity is present.

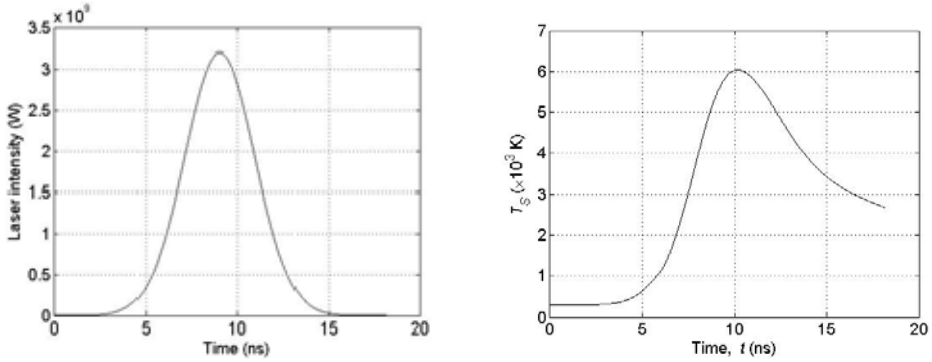

(a) (b)

Figs. 3. (a) Laser pulse intensity profile. (b) Temperature of the target surface.

The spatial distribution of the temperature and density of the ablation plume at different times relative to the onset of laser pulse is presented in Figs. 4(a,b). One can see in Fig. 4(a) that the maximum plume temperature of ~3500 K is reached at about 13 ns, 'long' after the peak of the laser pulse intensity. Fig. 4(b) depicts the spatial distribution of the plume density at different times. The figure indicates that a density of several 10^{19} cm^{-3}, which is suitable for efficient harmonic generation, can be obtained after the peak of the laser pulse at heights of several tens of microns above the target surface.

When the saturated vapor pressure (calculated by using Eq. (15)) becomes smaller that the pressure of the ablation plume (calculated by using previous data regarding density and temperature of the plume), the ablation velocity (calculated by using Eq. (14)) becomes negative and re-condensation begins.

From the continuity equation given by Eq. (19) we find that the local plume velocity near the target surface becomes also negative due to re-condensation process (see black curve in Fig. 4(c)). Thereby, the evaporation

depth, calculated by time integration of the evaporation velocity given by Eq. (14), decays when re-condensation comes into play at times larger than ~13 ns, when maximum of the plume temperature is reached (see Fig. 4(d)).

From graphs like those presented in Figs. 4 one can infer the correct positioning and timing of the HHG driving laser pulse within the conversion ablation plume so that to obtain phase matching conditions for different harmonics.

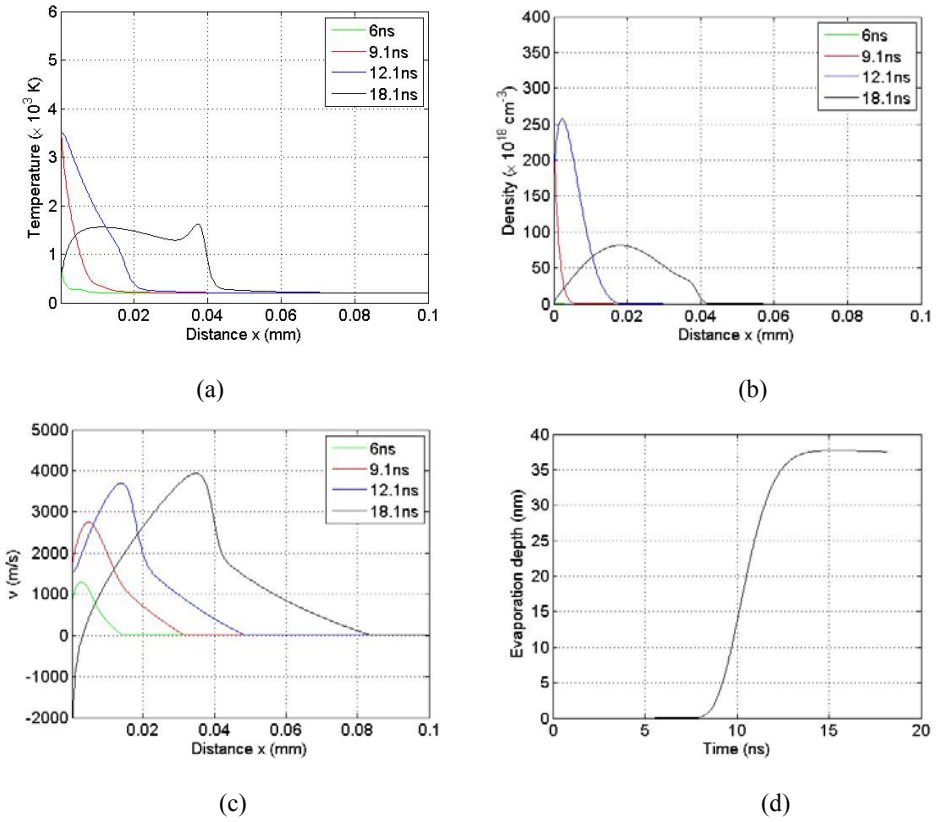

Figs. 4. (a) Spatial distribution of the ablation plume temperature at different irradiation times. (b) Spatial distribution of the ablation plume density at different times. (c) Spatial distribution of the ablation plume velocity at times. (d) Time dependent evaporation depth of the ablated target.

5. Conclusions

In this paper we present an analysis of high order harmonic generation in gas jets and also the evaluation of several parameters in order to obtain the highest conversion efficiency like: wave vector mismatches, concentrations of the gases,

length of the nonlinear medium and focusing parameters (focus length, beam radius at the waist).

The obtained parameters (wave vector mismatches, concentrations of the gases, length of the nonlinear medium and focusing parameters (focus length, beam radius at the waist) in the case of fifth and seventh order harmonics generation of a Nd^{3+}:YAG laser radiation in mixtures of sodium vapors and xenon are in good agreement with the experimental results published in the literature.

We also analyzed theoretically the properties of the ablation plumes conversion media produced with low intensity nanosecond laser pulses on Al targets in vacuum, in order to estimate the optimum conditions for HHG which are dependent on medium density and ionization degree.

Acknowledgements

This work was supported by a grant in the programme: CAPACITIES/RO-CERN, project type: ELI-NP, E/04 HHGDE, project number 04/27.06.2014.

R E F E R E N C E S

[1] *W. Boyd*, Nonlinear Optics, Academic Press Inc. 3rd Ed., Amsterdam, (2008).
[2] *R. A. Ganeev*, Nonlinear Optical Properties of Materials, Springer Series in Optical Sciences 174, DOI: 10.1007/978-94-007-6022-6_2, Springer Science+Business Media, Dordrecht (2013).
[3] *Mihai Stafe, Aurelian Marcu, Niculae N. Puscas*, Pulsed Laser Ablation of Solids, Basics, Theory and Applications, Springer Series in Surface Sciences, Volume 53, Series Editors: Gerhard Ertl, Berlin, Germany, Hans Lüth, Jülich, Germany, Douglas L. Mills, Irvine, USA, Springer Berlin Heidelberg, (2014).
[4] *I. V. Tomov and M. C. Richardson*, Fifth-harmonic generation in isotropic media, IEEE J. Quantum Electron., Vol. **12**, p. 521–531 (1976).
[5] *V. V Rostovtseva, A. P. Sukhorukov, V. G. Tunkin, and S. M. Saltiel*, Higher harmonics generation by cascade processes in focused beams, Optics Communications Vol. **22**, p. 56–60, (1977).
[6] *J. F Reintjes*, Nonlinear Optical Parametric Processes in Liquids and Gasses, Academic Press Inc., (1984).
[7] *I. M. Popescu, N. N. Puscas, P. E. Sterian,* Seventh Harmonic Generation by Focused Gaussian Beam in Isotropic Media, International Conference and School "Lasers and Application", Bucharest, Romania, 30 august - 11 september, 1982, LAICS, C. I. Press, Vol. **2**, p. 327-328, (1982).
[8] *V. L. Doitcheva, V. M. Mitev, L. I. Pavlov, K. V. Stamenov,* Efficient fifth order non-linear process by focused beam in metal vapour,. Optical and Quantum Electronis, Vol. 10, No. 2, p. 131-138, (1978).
[9] *D.C. Hanna, M.A. Yuratich, D. Cotter*, Nonlinear Optics of Free Atoms and Molecules, Springer, Berlin, (1979).
[10] *N Bloembergen,* Nonlinear Optics, Singapore: World Scientific, (1996).
[11] *M. Lopez-Arias et al*, Low-order harmonic generation in metal ablation plasmas in nanosecond and picosecond laser regimes, Journal of Applied Physics, 043111 (2012).

[12] *I. Lopez-Quintas*, Low-order harmonic generation in nanosecond laser ablation plasmas of carbon containing materials, Applied Surface Science 278 p. 33–37, (2013).
[13] *Y. Akiyama, K. Midorikawa, Y. Matsunawa, Y. Nagata, M. Obara, H. Tashiro, and K. Toyoda*, Phys. Rev. Lett. 69, 2176 (1992).
[14] *S. Kubodera et al*, Phys. Rev. A 48, 4576 (1993).
[15] *C.-G. Wahlstrom, S. Borgstrom, J. Larsson, and S.-G. Pettersson*, Phys. Rev. A 51, 585 (1995).
[16] *R. A. Ganeev, V. I. Redkorechev, and T. Usmanov*, Opt. Commun. 135, 251 (1997).
[17] *M. Stafe*, Theoretical photo-thermo-hydrodynamic approach to the laser ablation of metals, Journal of Applied Physics 112, 123112 (2012).
[18] *Mihai Stafe and Constantin Negutu*, Ablation plasma spectroscopy for monitoring in real-time the pulsed laser ablation of metals, Plasma Chemistry and Plasma Processing, Volume 32, Issue 3, Pages 643-653, (June 2012).
[19] *Zhaoyang Chen, Davide Bleiner, and Annemie Bogaerts*, Effect of ambient pressure on laser ablation and plume expansion dynamics: A numerical simulation, Journal of Applied Physics , 063304 (2006).
[20] *Andrey V. Gusarov, Alexey G. Gnedovets, and Igor Smurov*, Gas dynamics of laser ablation: Influence of ambient atmosphere, Journal of Applied Physics 88, 4352 (2000).
[21] *D.N. Patel, Ravi Pratap Singh, Raj K. Thareja*, Craters and nanostructures with laser ablation of metal/metal alloy in air and liquid, Applied Surface Science 288, p. 550– 557, (2014).
[22] *W. Marine, L. Patrone, B. Luk'yanchuk, M. Sentis*, Strategy of nanocluster and nanostructure synthesis by conventional pulsed laser ablation, Applied Surface Science 154–155, p. 345–352, (2000).
[23] *E.V. Barmina et al*, Laser-assisted generation of gold nanoparticles and nanostructures in liquid and their plasmonic luminescence, Appl. Phys. A 115, p.747–752, (2014).
[24] *Mihai Stafe, Constantin Negutu, Adrian Ducariu*, Pulsed laser ablated craters in aluminium in air and aqueous environments, Romanian Reports in Physics, Vol. 64, No. 1, P. 155–162 (2012).
[25] *Bauerle, D,* Laser processing and chemistry, Springer-Verlag, Berlin-Heidelberg-New York, (2000).
[26] *S. Zhang et al*, Laser-induced plasma temperature, Spectrochimica Acta - Part B Atomic Spectroscopy, 97, pp. 13-33 (2014).
[27] *J. Picard et al*, Characterization of laser ablation of copper in the irradiance regime of laser-induced breakdown spectroscopy analysis, Spectrochimica Acta - Part B Atomic Spectroscopy 101, pp. 164-170 (2014).
[28] *Nadezhda M.Bulgakova, Anton B.Evtushenko, Yuri G. Shukhov, Sergey I. Kudryashov, Alexander V. Bulgakov*, Role of laser-induced plasma in ultradeep drilling of materials by nanosecond laser pulses, Applied Surface Science 257, Issue 24, 10876-10882 (2011).
[29] *Deepak Marla, Upendra V. Bhandarkar, and Suhas S. Joshi*, Journal of Applied Physics, **109**, 02110 (2011).
[30] *Laszlo Balazs, Renaat Gijbels, Akos Vertes*, Expansion of Laser-Generated Plumes Near the Plasma Ignition Threshold, Analytical Chemistry 63, 314-320 (1991).
[31] *Zhaoyang Chen, Annemie Bogaerts*, Laser ablation of Cu and plume expansion into 1 atm ambient gas, Journal of Applied Physics 97, 063305 (2005).
[32] *R.D. Skeel, M. Berzins*, A Method for the Spatial Discretization of Parabolic Equations in One Space Variable, SIAM Journal on Scientific and Statistical Computing, Vol. 11, pp. 1-32 (1990).
[33] *B.Commercon, V. Debout, R. Teyssier*, A fast, robust, and simple implicit method for adaptive time-stepping on adaptive mesh-refinement grids, A&A 563, A11 DOI:10.1051/0004-6361/201322858, (2014).

[34] *P. W. Wachulak et al*, Extreme ultraviolet tomography of multi-jet gas puff target for high-order harmonic generation, Appl. Phys. B, 117:253–263 (2014).
[35] *A Willner et al*, Efficient control of quantum paths via dual-gas high harmonic generation, New J. Phys. 13 113001 (2011).
[36] *J. Cheng, W. Perrie, B. Wu, S. Tao, S. P. Edwardson, G. Dearden, K. G. Watkins*, Appl. Surf. Sci. 255, 8171–8175 (2009).